Neuroinform (2008) 6:23–34
DOI 10.1007/s12021-007-9006-6

ORIGINAL ARTICLE

Cortical Network Dynamics during Foot Movements

Fabrizio De Vico Fallani · Laura Astolfi · Febo Cincotti · Donatella Mattia · Maria Grazia Marciani · Andrea Tocci · Serenella Salinari · Herbert Witte · Wolfram Hesse · Shangkai Gao · Alfredo Colosimo · Fabio Babiloni

Received: 16 April 2007 / Accepted: 23 November 2007 / Published online: 12 February 2008

Abstract The present work intends to evaluate the dynamics of the cerebral networks during the preparation and the execution of the foot movement. In order to achieve this objective, we have used mathematical tools capable of estimating the cortical activity via high-resolution EEG techniques. Afterwards we estimated, the instantaneous relationships occurring among the time-series of sixteen regions of interest (ROIs) in the Alpha (7–12 Hz) and Beta (13–29 Hz) band through the adaptive multivariate autoregressive models. Eventually, we evaluated the weighted-topology of the cerebral networks by calculating some theoretical graph indexes. The results show that the main structural changes are encoded in the highest spectral contents (Beta band). In particular, during the execution of the foot movement the cingulate motor areas (CM) work as network "hubs" presenting a large amount of outgoing links to the other ROIs. Moreover, the connectivity pattern changes its structure according to the different temporal stages of the task. In particular, the communication between the ROIs reaches its highest level of efficiency during the preparation of the foot movement, as revealed by the "small-world" property of the network, which is characterized by the presence of abundant clustering connections combined with short average distances between the cortical areas.

Keywords High-resolution EEG · Adaptive MVAR · Granger causality · Graph theory

F. De Vico Fallani (✉) · A. Colosimo
Interdep. Research Centre for Models and Information Analysis in Biomedical Systems, University of Rome "Sapienza", Corso V. Emanuele, 244, 00186 Rome, Italy
e-mail: fabrizio.devicofallani@uniroma1.it

F. De Vico Fallani · L. Astolfi · F. Cincotti · D. Mattia · M. G. Marciani · A. Tocci · F. Babiloni
IRCCS "Fondazione Santa Lucia", Rome, Italy

A. Colosimo · F. Babiloni
Department of Human Physiology and Pharmacology, University "Sapienza", Rome, Italy

S. Salinari
Department of Computer and Systems Science, University "Sapienza", Rome, Italy

M. G. Marciani
Department of Neuroscience, University "Tor Vergata", Rome, Italy

H. Witte · W. Hesse
Institute of Medical Statistics Computer Sciences and Documentation, Friedrich Schiller University of Jena, Jena, Germany

S. Gao
Department of Biomedical Engineering, Tsinghua University, Beijng, China

Introduction

The necessity of an objective comprehension of the relationships among the different brain structures is assuming an essential role in Neuroscience (Horwitz 2003). Indeed, several methods with the aim of estimating the functional links among such structures have been proposed and discussed in literature (David et al. 2004; Lee et al. 2003). However, since the resulting connectivity patterns could have a relatively large size and a complex structure, the interpretation of these functional networks

remains an open issue. Consequently, there is a wide interest in the development and validation of mathematical tools that are appropriate to spot relevant features that describe those cerebral networks (Stam 2004; Salvador et al. 2005; Tononi et al. 1994; Sporns et al. 2004). The oscillatory behaviour of the brain's electrical activity indicates that frequency coding is one of the major candidates of its functioning (Basar 2004). Hence, many methods have been developed to estimate functional connections between brain areas in the frequency domain by using EEG or MEG recordings (David et al. 2004). Among these, the use of multivariate auto-regressive (MVAR) models for the estimation of cortical connectivity are particularly interesting as they characterize at the same time the direction and the spectral properties of the interaction between different cerebral signals and they require only one model to be estimated from all the time series (Kaminski and Blinowska 1991). However, the original definition of these methods requires the stationarity of the signals. Moreover the transitory transfer of causal information could remain hidden since a unique model is estimated on the whole time interval. On the other hand, brain connectivity is often modulated by rapid changes in time and frequency and the necessity to detect these dynamics has been recently underlined (Boccaletti et al. 2006). The stationarity hypothesis could bias the physiologic interpretation of the results obtained with the different frequency-based connectivity techniques available in literature.

Recently, other algorithms for the estimation of MVAR with time dependent coefficients have been developed in order to overcome this limitation (Ding et al. 2000; Moeller et al. 2001). In view of the fact that a graph is a mathematical representation of a network, which is essentially reduced to nodes and connections between them, a way to characterize the topological properties of the cerebral networks was proposed using a graph theoretical approach (Strogatz 2001; Sporns et al. 2004; Stam 2004). In particular, Watts and Strogatz (1998) proposed two characteristic measures, the average shortest path L and the clustering index C, to extract respectively the global and local properties of the network structure. They showed that graphs with many local connections (i.e. with a high C) and few random long distance connections (i.e. with a low L) identify a particular model that interpolate between a regular lattice and a random structure. Such models are designated as "small-world" networks in analogy with the concept of the small-world phenomenon observed more than 30 years ago in the social systems (Milgram 1967). Different types of real networks were shown to share these small-world features (Strogatz 2001; Stam 2004; Salvador et al. 2005). In the context of the brain connectivity these properties were demonstrated to reflect an optimal architecture for the information processing (Lago-Fernandez et al. 2000; Sporns et al. 2000). The large part of these studies often referred to unweighted and undirected networks. However, the empirical results demonstrate that purely topological models, which neglect weight and direction of the connections, are inadequate to explain the rich and complex properties observed in real systems (Boccaletti et al. 2006). According to this observation, some indexes were proposed for weighted and directed graphs in order to achieve the whole available information from the considered networks (Yook et al. 2001; Latora and Marchiori 2003).

The aim of this study is to evaluate the functional dynamics of the cortical network in every time-point during the preparation and the execution of the foot movement. This perspective seems relevant, since the large part of the current methods for the estimate of the functional connectivity return static relationships from fixed time-windows of brain activity. On the contrary, the change of direction and intensity of the functional links could point out some new insights about the transient processes that are supposed to occur among different specialized cortical areas and that cannot be observed by means of static or low-time resolution methods. In this study, the cortical connectivity is expected to rapidly change according to the different stages during the preparation and the execution of the foot movement.

Materials and Methods

EEG Recordings

Five voluntary and healthy subjects participated to the study (age, 26–32 years; five males). They had no history of neurological or psychiatric disorder, and they were free from medications, or alcohol or drug abuse. The informed consent statement was signed by each subject after the explanation of the study, which was approved by the local institutional ethics committee. For the EEG data acquisitions, the participants were comfortably seated on a reclining chair in an electrically shielded and dimly lit room. They were asked to perform a dorsal flexion of their right foot, whose preference was previously attested by simple questionnaires (Chapman et al. 1987). The movement task was repeated every 8 s, in a self-paced manner and 200 single trials were recorded by using 200 Hz of sampling frequency. A 96-channel system (BrainAmp, Brainproducts GmbH, Germany) was used to record EEG signals by means of an electrode cap and EMG electrical potentials through surface electrodes. In accordance to an extension of the 10–20 international system, the electrode cap was composed by 64 channels. The structural

MRIs of the subject's head were taken with a Siemens 1.5T Vision Magnetom MR system (Germany). Three dimensional electrode positions were obtained by using a photogrammetric localization (Photomodeler, Eos Systems Inc., Canada) with respect to the anatomic landmarks: nasion and the two pre-auricular marks. Some trained electroencephalographists visually inspected EEG data and all the trials containing artefacts were rejected. Subsequently, they were baseline adjusted and low-pass filtered at 45 Hz.

Estimation of the Cortical Activity

High-resolution EEG technologies have been developed to enhance the poor spatial information of the EEG activity (Le and Gevins 1993; Gevins et al. 1994; Nunez 1995). Principally, this technique involves the use of a large number of scalp electrodes (64–256), although this aspect is not its unique feature. Indeed, high-resolution EEG technologies use realistic MRI-constructed subject head models (Babiloni et al. 1997, 2000) and spatial de-convolution estimations which are commonly computed by solving a linear inverse problem based on boundary-element mathematics (Grave de Peralta Menedez and Gonzalez Andino 1999). In the present study, the cortical activity from EEG recordings was estimated by using a realistic head model whose cortical surface consisted of about 5,000 triangles uniformly disposed. The estimation of the current density strength for each triangle, which represents the electrical dipole of a particular neuronal population, was computed by solving the linear inverse problem according to techniques described in previous works (Babiloni et al. 2005; Astolfi et al. 2006). The electrical activity of different Regions of interest (ROIs) was obtained by averaging the current density of the various dipoles within the considered area.

The present experiment was based on sixteen regions of interest that were segmented from the cortical model of each subject. The ROIs considered for the left (_L) and right (_R) hemisphere are the primary motor areas of the foot (MF_L and MF_R), the proper supplementary motor areas (SM_L and SM_R) and the cingulate motor areas (CM_L and CM_R). The bilateral Brodmann areas 6 (6_L and 6_R), 7 (7_L and 7_R), 8 (8_L and 8_R), 9 (9_L and 9_R) and 40 (40_L and 40_R) were also considered. In order to inspect the brain dynamics during the preparation and the execution of the studied movement, a time segment of 2 s was analyzed, after having centred it on the onset detected by a tibial EMG. The most interesting cerebral processes concerning the detected movement are actually thought to occur within this interval (Pfurtsheller and Lopes da Silva 1999).

Time-varying Connectivity

The Partial Directed Coherence or PDC (Baccalà and Sameshima 2001) is a spectral measure used to determine the directed influences between any given pair of signals in a multivariate data set. As recently stressed (Kus et al. 2004), the multivariate approach avoids the problem of the estimation of spurious functional links, which is very common in conventional bivariate approaches like the spectral coherence. The PDC is obtained from a unique MVAR model estimated on the entire set of trials, according to the method proposed by Ding (Ding et al. 2000). The collection of EEG signals from these trials is treated as an ensemble of the realizations of a non-stationary stochastic process with locally stationary segments. In particular, if multiple performances of the same process are available, the method computes the covariance matrix of the whole set of EEG signals for each trial. Eventually the average across all the realizations give as result the final estimate of the covariance matrix. MVAR models have been already applied to cortical waveforms estimated from high-resolution EEG recordings, in order to achieve functional connectivity networks during cognitive and motor tasks, the latter in both normal subjects and spinal cord injured patients (Babiloni et al. 2005; Astolfi et al. 2005, 2006, 2007; De Vico Fallani et al. 2007b). The main limitation of this method in its paradigmatic formulation is the signal stationarity requirement within the examined period. In order to overcome this restriction, a time-varying formulation of PDC based on adaptive MVAR (aMVAR) models was thus employed in the present study. This measure is very interesting for estimating a connectivity pattern for each time-point and maintaining the same time resolution of the employed brain-imaging technique. The time-dependent parameter matrices were estimated by means of the recursive least squares algorithm with forgetting factor (RLS), as described in other studies (Moeller et al. 2001; Hesse et al. 2003). The multivariate Akaike's criterion was applied on each time sample and the highest order obtained was then utilised in all the recursive estimations. The order of the used aMVAR models ranged from 14 to 16 for all the experimental subjects.

Statistical Validation The rough connectivity estimation produces a full connected weighted and asymmetric matrix, representing the Granger-causal influences (Granger 1969) among all the cortical regions of interest. In order to consider only the task-related connections, a filtering procedure based on statistical validation was adopted. In each trial, a rest period of 2 s preceding the movement was selected as an element of contrast (from −4 to −2 s before the onset). The connection intensities regarding the pairs of ROIs for each time sample were collected in order to

obtain, a distribution of values belonging to the rest period. A threshold range was then extracted from the values of the rest-distribution by considering a percentile of 0.01 and 0.99, respectively, for the lowest and highest edge, with the aim of testing the significance of the estimated connections within the period of interest. After statistical filtering, the remaining weighted connections represent the significant relationships among the ROIs that characterize the experimental task.

Graph Analysis

A graph is an abstract representation of a network. It consists of a set of vertices (or nodes) and a set of edges (or connections) indicating the presence of some sort of interaction between the vertices. The adjacency matrix A contains the information about the connectivity structure of the graph. When a weighted and directed edge exists from the node i to j, the corresponding entry of the adjacency matrix is $A_{ij} \neq 0$; otherwise $A_{ij}=0$. In the four following paragraphs, we introduce the extension to time-varying analysis of several indices that have been used to characterize weighted and directed graphs.

Network Density The simplest attribute for a graph is its density k, defined as the actual number of connections within the model divided by its maximal capacity; density ranges from 0 to 1, the sparser is a graph, the lower is its value. When dealing with weighted networks, a useful generalization of this quantity is represented by the weighted-density k_w, which evaluates the intensities of the links composing the network. A time-varying formulation of this variable is given by the following:

$$k_w[A(t)] = \sum_{i \neq j \in V} w_{ij}(t) \tag{1}$$

Where $A(t)$ is the adjacency matrix at the time t and $w_{ij}(t)$ is the weight of the respective arc from the point j to the point i. $V = 1...N$ is the set of nodes within the graph. At each temporal point, the time-varying weighted-density gives information about the level of overall connectivity and constitutes the basis for correct analysis of all other graph parameters.

Node Strength In the same way, the simplest attribute of a node is its connectivity degree, which is the total number of connections with other vertices. In a weighted graph, the natural generalization of the degree of a node i is the node strength or node weight (Yook et al. 2001). This quantity has to be split into in-strength s_{in} and out-strength s_{out}, when directed relationships are considered. The strength index integrates the information of the links' number (degrees) with the connections' weight, thus representing the total amount of outgoing intensity from a node or incident intensity into it. The time-dependent formulation of the in-strength index s_{in} can be introduced as follows:

$$s_{\text{in}}(i,t) = \sum_{j \in V} w_{ij}(t) \tag{2}$$

It represents the whole functional flow incoming to the vertex i at the time t. V is the set of the available nodes and $w_{ij}(t)$ is the weight of the particular arc from the point j to the point i at the time t. In a similar way for the out-strength:

$$s_{\text{out}}(i,t) = \sum_{j \in V} w_{ji}(t) \tag{3}$$

It represents the whole functional flow outgoing from the vertex i at the time t. $w_{ji}(t)$ is the weight of the particular arc from the point i to the point j at the same time t.

Strength Distributions For a weighted graph, the arithmetical average of all nodes' strength $<s>$ gives little information about the distributions of the links intensity within the system. Hence, it is useful to introduce $R(s)$ as the fraction of vertices in the graph that have strength equal to s. In the same way, $R(s)$ is the probability that a vertex chosen uniformly at random has weight $=s$. Introducing the temporal variable, a plot of $R[s(t)]$ for any evolving network can be constructed by making a histogram of the vertices' strength for each time point. This histogram represents the strength distribution of the graph and allows a better understanding of the strength allocation in the system throughout time. In particular, when dealing with directed graphs, strength distribution has to be split in order to consider in a separated way the contribution of the incoming and outgoing flows.

Network's Structure Two measures are frequently used to characterize the local and global structure of unweighted graphs: the average shortest path L and the clustering index C (Watts and Strogatz 1998; Newman 2003; Grigorov 2005). The former measures the efficiency of the passage of information among the nodes, the latter indicates the tendency of the network to form highly connected clusters of nodes. Recently, a more general setup has been examined in order to investigate weighted networks (Boccaletti et al. 2006). In particular Latora and Marchiori (2001) considered weighted networks and defined the efficiency coefficient e of the path between two vertices as the inverse of the shortest distance between the vertices (note that in weighted graphs the shortest path is not

necessarily the path with the smallest number of edges). In the case where a path does not exist, the distance is infinite and $e=0$. The average of all the pair-wise efficiencies e_{ij} is the global-efficiency E_{glob} of the graph. The time-varying global-efficiency can be defined as:

$$E_{\text{glob}}[A(t)] = \frac{1}{N(N-1)} \sum_{i \neq j \in V} \frac{1}{d_{i,j}(t)} \tag{4}$$

where N is the number of vertices composing the graph.

Since the efficiency e also applies to disconnected graphs, the local properties of the graph can be characterized by evaluating for every vertex i the efficiency coefficients of A_i, which is the sub-graph composed by the neighbours of the node i. Thus, the time-varying local-efficiency E_{loc} is the average of all the sub-graphs global-efficiencies computed at the time t:

$$E_{\text{loc}}[A(t)] = \frac{1}{N} \sum_{i \in V} E_{\text{glob}}[A_i(t)] \tag{5}$$

Since the node i does not belong to the sub-graph A_i, this measure reveals the level of fault-tolerance of the system, showing how the communication is efficient between the first neighbours of i when i is removed. Global- (E_{glob}) and local-efficiency (E_{loc}) were demonstrated to reflect the same properties of the inverse of the average shortest path $1/L$ and the clustering index C (Latora and Marchiori, 2003). Hence, the definition of small-world can be rephrased and generalized in terms of the efficiency indexes (Boccaletti et al. 2006; Stam and Reijneveld 2007). Small-world networks have high E_{glob} (i.e. high $1/L$) and high E_{loc} (i.e. high C). This original definition seems to be attractive since it takes into account the full information contained in the weighted links of the graph and provides an elegant solution to handle disconnected vertices.

In the following we will refer to the inverse of the average shortest path $1/L$ and to the clustering index C, since in general the term "efficiency" implies some a-priori interpretation depending really on what the graph models. It is worth to mention that in the present study the term "communication" stands for the existence of functional links between ROIs, estimated in specific frequency bands during the preparation and the execution of a simple movement.

Contrast with Random Graphs All the indexes calculated on the cortical networks were standardized by considering their Z-score with respect to the distribution obtained from 50 random graphs. For each frequency band and time-sample, random patterns were generated from the cerebral network of each subject, by shuffling the connections and maintaining the same in- and out-degree, but not the same strength. (Sporns and Zwi 2004)

Group Analysis A common number of connections (or density) has been considered in each weighted graph in order to analyze the structure of the cortical networks across all the subjects, frequency bands and time samples. In fact, when seeking a common behaviour among different networks, the mathematical indexes that evaluate their properties could suffer in robustness when they apply to graphs with different densities. Consequently, this study will take into consideration 48 connections (i.e. density= 0.2) for each network obtained by removing the weakest links from each weighted graph. The choice of this connection-density was surely the most favourable condition for the significance of the indexes of the network structure ($1/L$ and C). At a more specific analysis, it has been found that these indexes keep their usual independency—characterized by their ability to detect global and local properties—even in a small 16 nodes-graph (data not shown here).

Results

Figure 1 presents on the left a superimposition of the electrode montage with the actual head structures for a representative subject, as an example for the different steps involved in the estimation of the high resolution EEG signals obtained in this study. The locations of the regions of interest (ROIs) are illustrated in colour on the left hemisphere of the cortex together with their estimated temporal activity.

Figure 1 also shows the time-varying power spectrum densities (PSD) for the ROIs of the representative subject. They have been computed by means of the same MVAR model employed in the estimation of the evolving connectivity patterns. The time–frequency maps reveal the typical drop of spectral power during the neuron desynchronization (Pfurtscheller and Lopes da Silva 1999), which occurs in the motor areas in proximity of the execution of the movement, especially in the Alpha (7–12 Hz) and Beta (13–29 Hz) frequency bands. As described above, the use of the time-varying Partial Directed Coherence (PDC) on the cortical waveforms obtained from EEG signals returns a cortical network for each selected time sample and frequency. In the present work, we focused our analysis on two particular spectral ranges related to the movement, specifically the Alpha and Beta band. In fact, those frequency bands have been suggested to be the most responsive channels to the preparation and execution of a simple limb movement (Pfurtscheller and Lopes da Silva

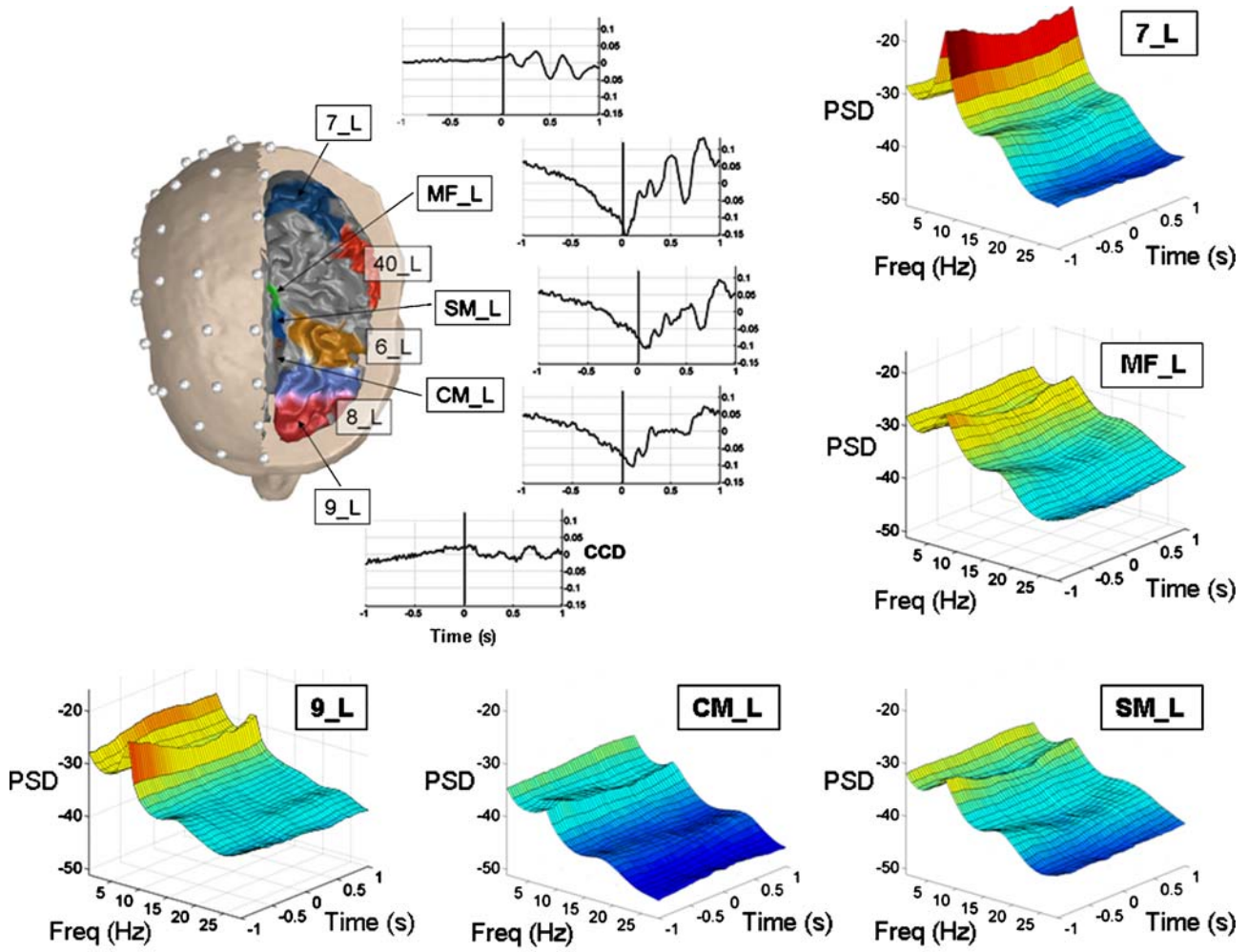

Fig. 1 Realistic head model for the representative subject. On the right hemisphere of the scalp the positions of the electrodes are depicted as *white little spheres*. On the left hemisphere of the cortex all the cortical regions of interest are displayed in colour and opportunely labelled. The trial-averaged waveforms (Cortical Current Density) for a particular subset of areas (7_L, MF_L, SM_L, CM_L, 9_L) are illustrated together with their time-varying Power Spectrum Density (PSD in decibel)

1999). Figure 2a shows the average connectivity patterns in three particular moments for the representative Beta frequency band. In particular, each network shows the average intensity of the connections that are in common at least to three subjects.

In this figure, one arrow from the node *X* to the node region *Y* indicates the existence of a statistically significant Granger causality relationship between the cortical areas they are representing. The time-varying strength indexes computed for each subject have been contrasted with the values obtained from the respective random structures, to be able to return a statistical significance (see "Materials and Methods"—"Graph Analysis"). As regards the time points preceding (about −560 ms) and following (about + 920 ms) the movement onset, the functional network of the subjects showed a configuration that is very different from the relevant random structure, as revealed by the general high *Z* values of their strength indexes. In particular, intense functional links from the cingulate motor areas of both the hemispheres (CM_L and CM_R) to the supplementary motor areas (SM_L and SM_R) can be observed during all the three considered moments. Figure 2b shows the in-strength values for the average network during the three moments of interest previously considered in Fig. 2a. Among all the cortical regions, the supplementary motor areas of both hemispheres (SM_L and SM_R) show the highest values of in-strength index. In the time points that precedes the onset movement (−560 ms) also the right and left primary motor areas of the foot (MF_L and MF_R) present a considerable number of incoming functional links. Figure 2c shows the average values of out-strength obtained during the three time points of interest estimated from the graphs showed in Fig. 2a. In this particular case, it is evident that the large part of the cortical areas does not produce outgoing edges, while the bilateral cingulate motor region (CM_L and CM_R) presents very high out-strength values. The whole

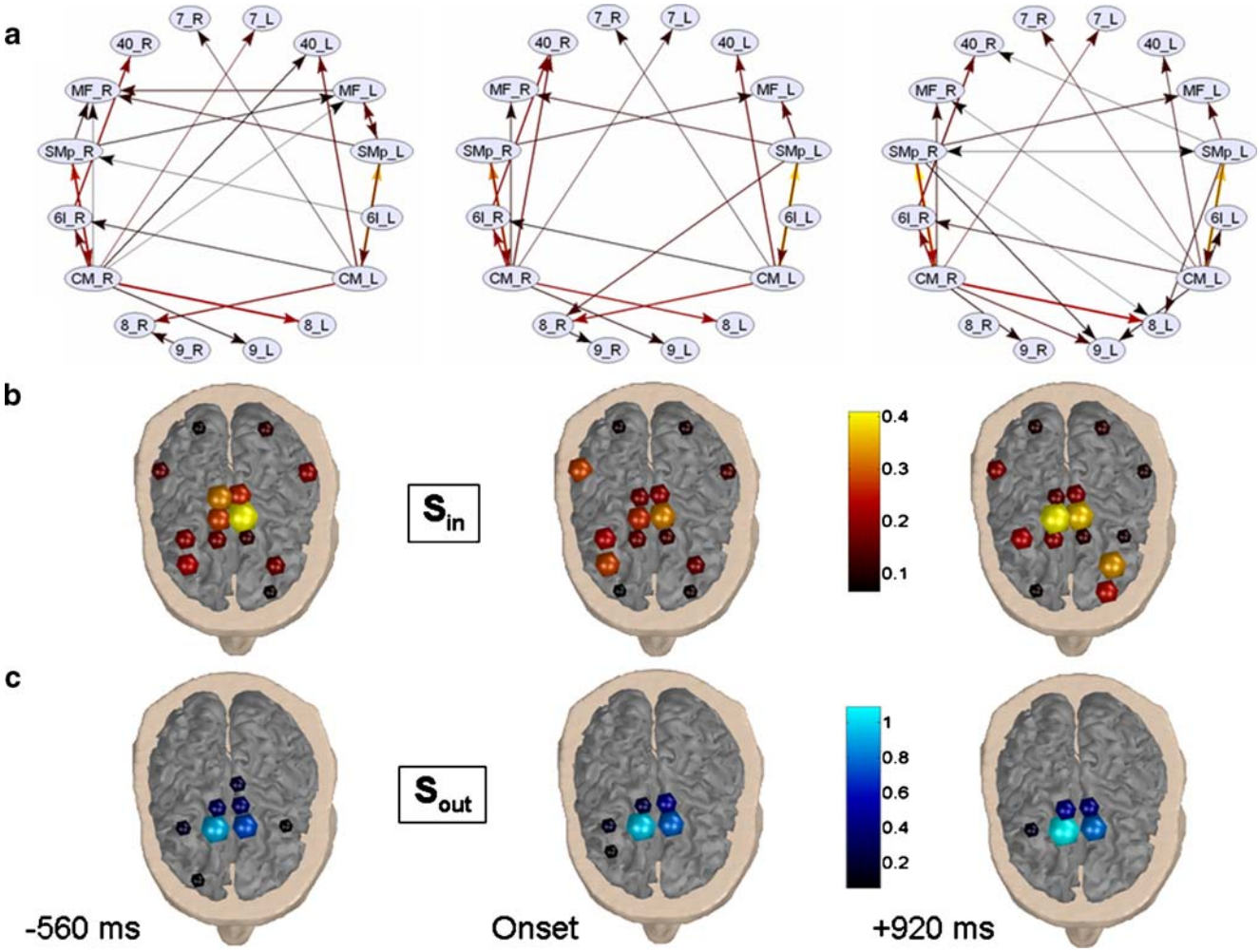

Fig. 2 **a** Representation of the average networks in the Beta frequency band during three characteristic instants. Each pattern shows the average intensity of the connections that are common to three subjects at least. The Granger-causality from an area *X* to *Y* is represented by an *arrow*; the intensity of this relationship is coded by its size and colour. The lighter and bigger is the *arrow*, the higher is the intensity. **b** Values of "in-strength" $S_{in}(t)$ for the average networks in the Beta band during the same instants. The functional flow, which incomes into each region of interest, is represented on the cortex by a *sphere* localized in correspondence to the barycentre of the respective area. The intensity of the index is encoded by the size and colour of each *sphere*. The lighter and bigger is the sphere, the higher is the strength. **c** "Out-strength" $S_{out}(t)$ for the Beta band. Same conventions as in **b**. The absence of spheres in correspondence of some ROIs means lack of outgoing links

time progress of the strength indexes during the analyzed period of interest (2 s) was inspected for each subject and frequency band. Figure 3 shows the average *Z*-scores of the in- and out-strength indexes obtained from the analyzed population in the Beta band. In this figure only the ROIs presenting a significant behaviour during the entire period are illustrated.

It is remarked that throughout the large part of the movement execution, the in-strength values of the cingulate (CM_L, CM_R) and supplementary (SM_L, SM_R) motor areas are significantly ($p<0.01$) higher than the ones obtained from a random re-distribution of the links. As regards the out-strengths, only the CM_L and CM_R presented a significant higher level of involvement when compared with the random graph. The analysis of the Alpha band allowed us to draw similar conclusions about the persistently high ($p<0.01$) values of in- and out-strength in both the CM areas; in opposition with the Beta band, both the SM regions did not show statistically significant values (data not shown here).

It is necessary to compute the distributions of the strengths of the estimated functional cortical networks in order to achieve a more detailed analysis. The examined distribution represents the fraction of vertices in the graph that have strength equal to a value *s*. The distributions of each subject have been contrasted with the ones obtained from the respective random networks in order to test their significance (see "Materials and Methods"—"Contrast with Random Graphs"). In particular, for each time point we contrasted the histograms of the strength distribution

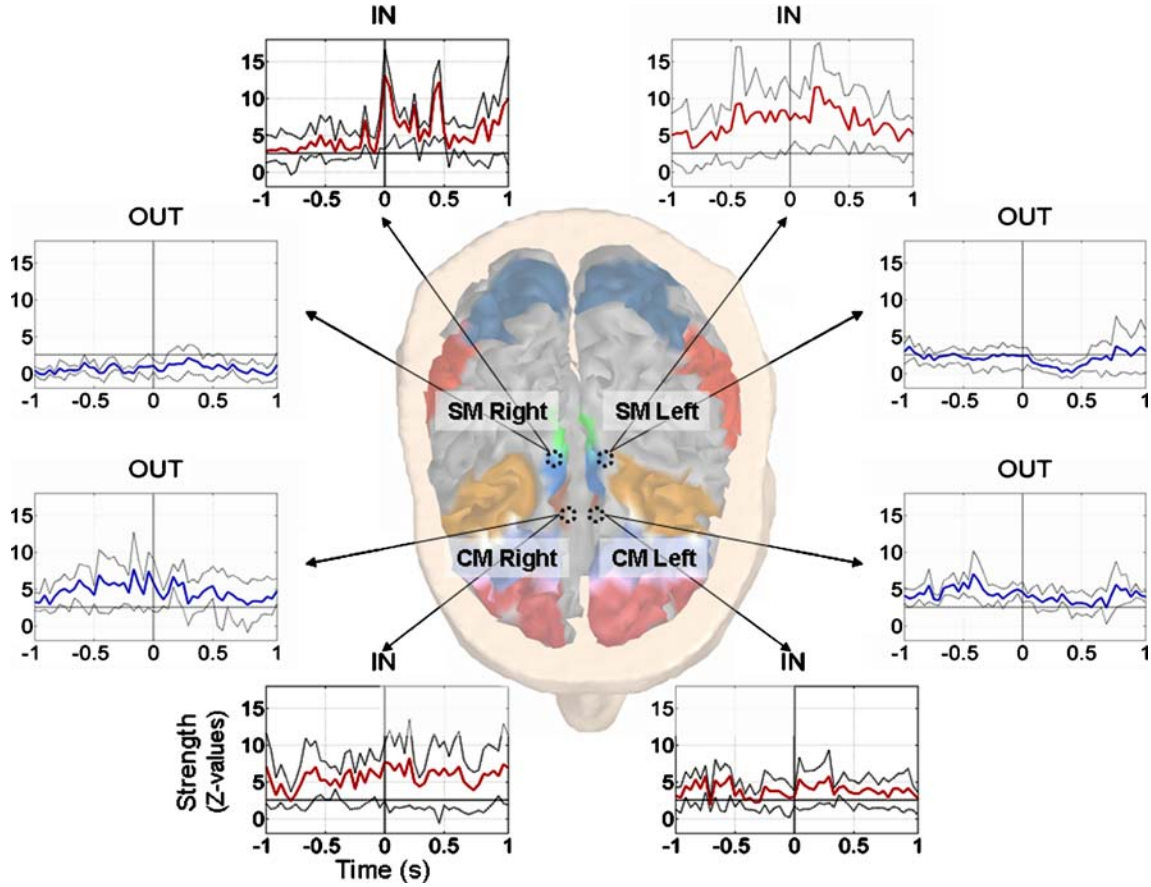

Fig. 3 Representation of the time-varying "strengths" for a group of ROIs in the Beta band. Each sub-plot describes the evolving behaviour of a particular region within the cortical network and during the entire period of the task. The latency from the movement onset is shown on the *X*-axes. *Red* or *blue lines* represent the average of the in- or out-strength *Z*-scores obtained from all the subjects. The lighter lines around the mean value indicate the profiles of the 25th and 75th percentile

between the cortical and the random network. Figure 4 shows the average Z values in the analyzed population for the time-varying in- strength $R_{in}(t)$ and out-strength $R_{out}(t)$ distributions in the Beta frequency band.

The latency from the onset movement is represented on the abscissas of the figure, while on the ordinates the strength bins of the histograms previously computed are scored. The colour encodes the intensity of the computed Z value for the R index that measures how much the fraction of ROIs, having at a particular time t a strength equal to s, is different from a random configuration. An interesting result is that in-strength (R_{in}) and out-strength (R_{out}) distributions show different characteristics. In fact, as shown in Fig. 4b the R_{out} index reveals statistically significant ($p<0.01$) differences from the random case. The high Z-scores in correspondence with the high values of S_{out} (i.e. the "right tail" of the distribution) suggest the presence of few ROIs with a very high level of outgoing flows, which makes them act as cortical "hubs." In particular, the intensity of their outgoing links seems to increase as time elapses from the movement preparation to the movement execution, as revealed by the respective shift of the significant Z values towards high levels of out-strength. The general distribution of the incoming flows within the functional network does not present significant differences from a random behaviour. In fact, inspecting Fig. 4a it is evident that the overall Z-scores of R_{in} are not statistically significant (with many values between −1.96 and 1.96). These low values of Z suggest that the in-strength distributions of the estimated cortical networks for the movement preparation and execution have the same profile as the distributions computed from the random graphs, which are known to show a uniform distribution of their flows and the absence of "hubs." Analogous results were observed in the Alpha frequency band where only the average out-strength distributions showed significant Z-scores in correspondence with their tails (data not shown here).

As described in the "Materials and Methods," the level of organization in the time-varying cortical networks during the foot movement was analyzed by computing the efficiency coefficient e. On a global scale, this index was employed for calculating the inverse of the average shortest path $1/L$ that measures the "overall communication" among

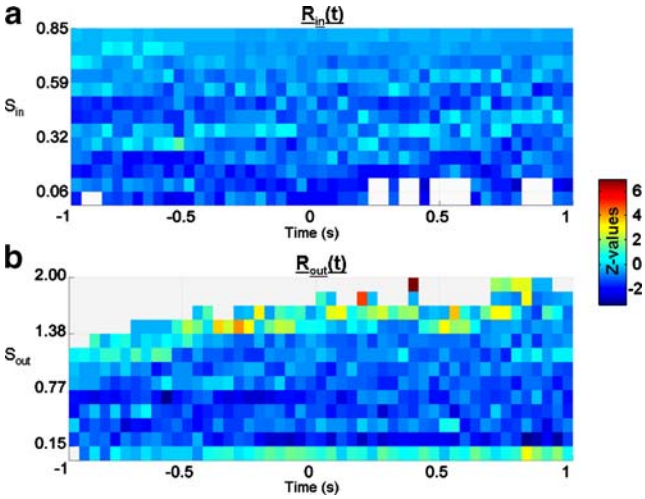

Fig. 4 **a** Representation of the time-varying "in-strength distributions" $R_{in}(t)$ during the period of interest in the Beta band. The latency from the movement onset is shown on the *X*-axes; the in-strength (S_{in}) values on the *Y*-axes. The colour encodes the group-averaged intensity of the R_{in} *Z*-score. In particular the *light grey colour* stands for the absence of ROIs with $S_{in}>0$ at the instant *t*. **b** The group-averaged *Z*-scores of the "out-strength distributions" $R_{out}(t)$ in the Beta band, represented in accordance with the previous conventions

the units of the network. On a local scale, the efficiency coefficient gives as a result the measure for the clustering index *C* that represents the tendency of the network to form clusters that mutually share functional connections. The $1/L$ and *C* indexes estimated in every subject from the respective cortical networks were contrasted with the ones obtained from the respective random structures. It is worth to mention that among the possible network configurations, random graphs have the highest values of the inverse of the average shortest path and the lowest values of the clustering index. Therefore, high values of $1/L$ will be assessed when the respective *Z*-score is not significant ($p\geq0.05$). On the contrary the high values of *C* will be assessed when the respective *Z* is significantly ($p<0.05$) higher than random patterns. Figure 5a shows the average *Z*-scores of the time-varying $1/L$ (blue line) and *C* (red line) of the connectivity patterns in the Beta frequency band.

Table 1 summarizes in a schematic way the average behaviour of the indexes obtained during the task performance of the analyzed population. In particular, 1 s before the onset movement (from about −1 to −0.5 s), the cortical networks mostly show low values of $1/L$ and *C*. Throughout the period closer to the execution of the movement (from about −0.5 s to the onset), both the global and local properties increase and in correspondence with it, we observe high values of $1/L$ and *C*. After the onset (from the onset to +0.5 s), the estimated cortical networks still present high values of $1/L$ but not with *C*, whose values lower significantly. In the last part (from about +0.5 to +1 s) of the movement execution the *C* index is in general high, while the $1/L$ index follows a decreasing slope with rather low values. The analysis of the structure indexes $1/L$ and *C* in the Alpha band did not reveal a particular sequence of different network configurations. Indeed the estimated connectivity patterns showed a constant time-course of low $1/L$ and high *C* during the preparation and the execution of the foot movement (data not shown here).

Figure 5b shows the average time-varying course of the weighted-density k_w in the Beta band during the analyzed period of interest. In general, a progressive increase of k_w can be observed as time approaches the onset movement, although a short and rapid decay occurs at about 500 ms after the onset movement. The behaviour of the average weighted-density in the Alpha band showed a highest level of overall connectivity with respect to the Beta spectral content (data not shown here) and a progressive increase from the preparation to the movement execution, as observed in the Beta band.

Discussion

This work aims at evaluating the functional dynamics of the cortical networks during the moments characterizing the preparation and the execution of the foot movement. Some indexes deriving from graph theory have been applied to the time-varying networks estimated from a set of high-resolution EEG data in a group of healthy subjects. Application of graph theory to small networks is rather new if compared to its usual employment in biological context. However, the need for the analysis of small cerebral networks has been recently underlined (Hilgetag et al. 2000; Micheloyannis et al. 2006; Stam et al. 2006a, b). We would like to emphasize that the opportunity to deal with cortical activity permits the representation of the graph nodes as particular Brodmann areas on the cortex (Babiloni et al. 2005; De Vico Fallani et al. 2007a). The use of raw EEG signals instead returns less powerful results, since the nodes within the network represent scalp electrodes, which could have indirect links with the cortical areas beneath them. In this context, the adaptive Partial Directed Coherence could represent a major improvement in the analysis and interpretation of EEG and MEG data. In fact, the possibility to deal explicitly with weighted and asymmetric relationships as well as the observation of transient couplings would provide the analytical tools to observe the specific cortical network dynamics during the task. In order to limit the discussion of the results, the present study has analyzed the cortical networks in the Alpha (7–12 Hz) and Beta (13–29 Hz) frequency band representing the spectral contents principally involved in the preparation and the execution of simple motor acts (Pfurtsheller and Lopes da Silva 1999). However, this

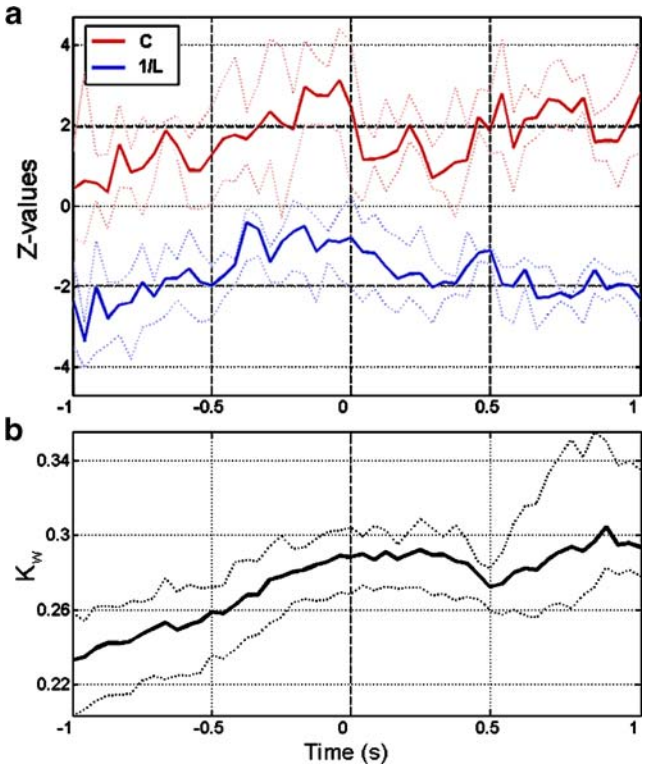

Fig. 5 **a** Time courses of the indexes for the network structure. *Blue lines* represent the average *Z*-scores for the inverse of the average shortest path $1/L$. *Red lines* represent the average *Z*-scores for the clustering index *C*. The *lighter lines* around the mean value indicate the time courses of the 25th and 75th percentile. The latency from the movement onset is shown on the *X*-axes. **b** Time-varying "weighted-density" during the whole time period in the Beta band. It represents the average *Z*-scores of the $k_w(t)$ indexes obtained from all the subjects with the same conventions as in **a**

methodology is not limited to a particular frequency band or a particular set of ROIs, since it can be adapted to investigate experimental tasks in any spectral content.

The successful execution of a simple movement relies on the integrated neural activity in spatially distributed networks, which encompass several frontal pre-motor, primary sensorimotor and subcortical structures (Ohara et al. 2001). As regards the Alpha and Beta band, the strong functional links between the cingulate motor (CM_L and CM_R) areas and the supplementary motor (SM_L and SM_R) areas are expected to be involved in a self-paced modality of movement generation, exactly as in our experimental condition (Gerloff et al. 1998). Indeed, the bilateral SM in the Alpha and Beta band and the CM areas in the Beta band showed a persistent involvement throughout the entire considered period. The significant ($p<0.01$) differences with respect to a random re-distribution of the links reveal the characteristic role of such regions. In particular, the SM areas represent the main target for a large number of functional connections taking origin from the other investigated cortical areas. In addition, the CM_L and CM_R represent the main sources of outgoing flows towards all the other ROIs, as revealed by the high statistical significance of their out-strength indexes.

Beyond the simple evaluation of the estimated functional flow intensities in different cortical areas, the strength distribution gave additional information about the allocation of these flows within the modelled cortical system. The average time-varying profiles reveal a different behaviour between the distributions of the incoming and outgoing strength indexes in the Alpha and Beta band. In fact, the out-strength distribution only indicates a significant ($p<0.01$) presence of few cortical areas—i.e. the nodes of the modelled graph—acting as "hubs," characterized by a very high level of outgoing functional flows. Looking more closely at the strength values of the ROIs previously analyzed, the cingulate motor areas (CM_L and CM_L) are found to act as the centre of outgoing flows for the estimated cortical functional network. This fact suggests a central role of these regions in both the considered spectral contents, since their removal would immediately corrupt the organization of the estimated functional network by reducing the overall level of connectivity. It is interesting to remark that only in the Beta band this specific involvement increases during the execution of the foot movement, which indicates a predominant role of the CM areas in this period and spectral content.

Finally, the study of the structural properties of the graph, evaluated by the clustering index *C* and the inverse of the average shortest path $1/L$ was performed by calculating the local-efficiency E_{loc} and the global-efficiency E_{glob} (see "Materials and Methods"). The results in the Beta band revealed the succession of different functional architectures during the preparation and the execution of the foot movement. In particular, 1 s before the onset movement (from about −1 to −0.5 s), the cortical networks mostly show low values of $1/L$ and *C*, which reflects a weak pattern of communication characterized by long average distances and few clustering connections between the ROIs. The closer the execution of the movement is (from about −0.5 s to the onset), the more both $1/L$ and *C*

Table 1 Average profiles of $1/L$ and C during the different stages of the foot movement

	−1.5→−0.5 s	−0.5 s→onset	onset→+0.5 s	+0.5→+1 s
$1/L$	↓*	↑	↑	↓*
C	↓	↑*	↓	↑*

The pointing upward arrow indicates an increase of the respective value of the parameter and viceversa. The asterisk means that the increase/decrease is significantly different from random networks ($p<0.05$).

increase. Consequently the structure of the cortical networks tends to maximize the interplay between the global integration and its local interactions. This particular structure represents one of the best way in which the cortical areas communicate, since the relevant network presents simultaneously short links between each pair of ROIs and highly connected clusters—i.e. small-world architecture (Watts and Strogatz 1998). After the onset (from the onset to+0.5 s), the estimated cortical networks show a typical random organization of the functional links (Watts and Strogatz 1998), with a high $1/L$ and a low C, reflecting the dense presence of wide-scope interactions among the ROIs, but a low tendency of the same cortical regions to form functional clusters. In the last period of the movement execution (from about +0.5 to +1 s) the estimated cortical networks mainly show high C values and low $1/L$ values. The resulting structure is known to reflect the properties of regular and ordered graphs (Watts and Strogatz 1998) in which the local property of clustering is privileged with respect to the overall communication. In the Alpha band, the network structure seems to follow a stationary profile, since the inverse of average shortest path and the clustering index remain quite constant during the entire analyzed period. In particular, the functional networks hold a regular configuration independently from the cortical dynamics that characterized the task, which indicates that main network changes are encoded in the higher spectral frequencies (Beta band). In addition to the efficiency analysis, the evaluation of the average weighted-density k_w associated to the evolution of the cortical network returned further information regarding the varying level of overall connectivity. In the Beta band, the average intensity of the network links during the preparation (from −0.5 s to the onset) is relatively low if compared with its maximum value reached in the following movement execution. In correspondence with this period the network structure presents the most efficient pattern of communication, as revealed by the estimated small-world characteristic. Therefore, it is interesting to note that the optimal organization of the functional links among the cortical areas during the preparation of the foot movement is not correlated to the need of a high level of overall connectivity.

Altogether, our findings revealed new insights about the time–frequency dynamics of the cortical networks involved throughout the performance of a simple foot movement. In particular, the adaptation of theoretical graph approaches to the time-varying connectivity showed that the functional dynamics of the cortical network can be detected through non-invasive neuroelectrical measurements. Eventually it is worth to remark that the temporal features of the evolving cortical network would not be detectable through some static or low-time resolution methods.

Information Sharing Statement

At the moment, all the resources utilized in the present work are not accessible by the general public.

Acknowledgment The present study was performed with the support of the COST EU project NEUROMATH (BMB 0601), of the Minister for Foreign Affairs, Division for the Scientific and Technologic Development, in the framework of a bilateral project between Italy and China (Tsinghua University) and the support of the European Union, through the MAIA project, the European IST Programme FET Project FP6-003758 and by the German Research Foundation (DFG Priority Program SPP 1114, LE 2025/1-3). This paper only reflects the authors' views and funding agencies are not liable for any use that may be made of the information contained herein.

References

Astolfi, L., Cincotti, F., Babiloni, C., Carducci, F., Basilisco, A., Rossini, P. M., et al. (2005). Estimation of the cortical connectivity by high resolution EEG and structural equation modeling: Simulations and application to finger tapping data. *IEEE Transactions on Biomedical Engineering*, *52*(5), 757–768.

Astolfi, L., Cincotti, F., Mattia, D., Marciani, M. G., Baccalà, L., De Vico Fallani, F., et al. (2006). A comparison of different cortical connectivity estimators for high resolution EEG recordings. *Human Brain Mapping*, *28*(2), 143–157.

Astolfi, L., De Vico Fallani, F., Cincotti, F., Mattia, D., Marciani, M. G., Bufalari, S., et al. (2007). Imaging functional brain connectivity patterns from high-resolution EEG and fMRI via graph theory. *Psychophysiology*, *44*(6), 880–893.

Babiloni, F., Babiloni, C., Carducci, F., Fattorini, L., Anello, C., Onorati, P., et al. (1997). High resolution EEG: a new model-dependent spatial deblurring method using a realistically-shaped MR-constructed subject's head model. *Electroencephalography and Clinical Neurophysiology*, *102*, 69–80.

Babiloni, F., Babiloni, C., Locche, L., Cincotti, F., Rossini, P. M., & Carducci, F. (2000). High resolution EEG: source estimates of Laplacian-transformed somatosensory-evoked potentials using a realistic subject head model constructed from magnetic resonance images. *Medical & Biological Engineering & Computing*, *38*, 512–519.

Babiloni, F., Cincotti, F., Babiloni, C., Carducci, F., Basilisco, A., Rossini, P. M., et al. (2005). Estimation of the cortical functional connectivity with the multimodal integration of high resolution EEG and fMRI data by Directed Transfer Function. *Neuroimage*, *24*(1), 118–113.

Baccalà, L. A., & Sameshima, K. (2001). Partial Directed Coherence: a new concept in neural structure determination. *Biological Cybernetics*, *84*, 463–474.

Basar, E. (2004). *Memory and brain dynamics: oscillations integrating attention, perception, learning and memory* p. 261. Boca Raton, FL: CRC.

Boccaletti, S., Latora, V., Moreno, Y., Chavez, M., & Hwang, D. U. (2006). Complex networks: structure and dynamics. *Physics Reports*, *424*, 175–308.

Chapman, J. P., Chapman, L. J., & Allen, J. J. (1987). The measurement of foot preference. *Neuropsychologia*, *25*(3), 579–584.

David, O., Cosmelli, D., & Friston, K. J. (2004). Evaluation of different measures of functional connectivity using a neural mass model. *Neuroimage*, *21*(2), 659–673.

De Vico Fallani, F., Astolfi, L., Cincotti, F., Mattia, D., Marciani, M. G., Salinari, S., et al. (2007b). Cortical functional connectivity networks in normal and spinal cord injured patients: Evaluation by graph analysis. *Hum Brain Mapping*, *28*, 1334–1336.

De Vico Fallani, F., Astolfi, L., Cincotti, F., Mattia, D., Tocci, A., Marciani, M. G., et al. (2007a). Extracting information from cortical connectivity patterns estimated from high resolution EEG recordings: A theoretical graph approach. *Brain Topography*, *19* (3), 125–136.

Ding, M., Bressler, S. L., Yang, W., & Liang, H. (2000). Short-window spectral analysis of cortical event-related potentials by adaptive multivariate autoregressive modeling: data preprocessing, model validation, and variability assessment. *Biological Cybernetics*, *83*, 35–45.

Gerloff, C., Richard, J., Hadley, J., Schulman, A. E., Honda, M., & Hallett, M. (1998). Functional coupling and regional activation of human cortical motor areas during simple, internally paced and externally paced finger movements. *Brain*, *121*, 1513–1531.

Gevins, A., Le, J., Martin, N., Brickett, P., Desmond, J., & Reutter, B. (1994). High resolution EEG: 124-channel recording, spatial deblurring and MRI integration methods. *Electroencephalography and Clinical Neurophysiology*, *39*, 337–358.

Grigorov, M. G. (2005). Global properties of biological networks. *DDT*, *10*, 365–372.

Granger, C. W. J. (1969). Investigating causal relations by econometric models and cross-spectral methods. *Econometrica*, *37*, 424–438.

Grave de Peralta Menendez, R., & Gonzalez Andino, S. L. (1999). Distributed source models: standard solutions and new developments. In C. Uhl (Ed.) *Analysis of neurophysiological brain functioning* (pp. 176–201). Berlin: Springer.

Hesse, W., Möller, E., Arnold, M., & Schack, B. (2003). The use of time-variant EEG Granger causality for inspecting directed interdependencies of neural assemblies. *Journal of Neuroscience Methods*, *124*, 27–44.

Hilgetag, C. C., Burns, G. A. P. C., O'Neill, M. A., Scannell, J. W., & Young, M. P. (2000). Anatomical connectivity defines the organization of clusters of cortical areas in the macaque monkey and the cat. *Philosophical Transactions of the Royal Society of London. Series B, Biological Sciences*, *355*, 91–110.

Horwitz, B. (2003). The elusive concept of brain connectivity. *Neuroimage*, *19*, 466–470.

Kaminski, M., & Blinowska, K. (1991). A new method of the description of the information flow in the brain structures. *Biological Cybernetics*, *65*, 203–210.

Kus, R., Kaminski, M., & Blinowska, K. J. (2004). Determination of EEG activity propagation: pair-wise versus multichannel estimate. *IEEE transactions on Biomedical Engineering*, *51*(9), 1501–1510.

Lago-Fernandez, L. F., Huerta, R., Corbacho, F., & Siguenza, J. A. (2000). Fast response and temporal coherent oscillations in small-world networks. *Physical Review Letters*, *84*, 2758–2761.

Latora, V., & Marchiori, M. (2001). Efficient behaviour of small-world networks. *Physical Review Letters*, *87*, 198701.

Latora, V., & Marchiori, M. (2003). Economic small-world behaviour in weighted networks. *European Physical Journal B*, *32*, 249–263.

Le, J., & Gevins, A. (1993). A method to reduce blur distortion from EEG's using a realistic head model. *IEEE Transactions on Biomedical Engineering*, *40*, 517–528.

Lee, L., Harrison, L. M., & Mechelli, A. (2003). The functional brain connectivity workshop: Report and commentary. *Neuroimage*, *19*, 457–465.

Micheloyannis, S., Pachou, E., Stam, C. J., Vourkas, M., Erimaki, S., & Tsirka, V. (2006). Using graph theoretical analysis of multi channel EEG to evaluate the neural efficiency hypothesis. *Neuroscience Letters*, *402*, 273–277.

Milgram, S. (1967). The small world problem. *Psychology Today*, pp 60–67.

Moeller, E., Schack, B., Arnold, M., & Witte, H. (2001). Instantaneous multivariate EEG coherence analysis by means of adaptive high-dimensional autoregressive models. *Journal of Neuroscience Methods*, *105*, 143–158.

Newman, M. E. J. (2003). The structure and function of complex networks. *SIAM Review*, *45*, 167–256.

Nunez, P. L. (1995). *Neocortical dynamics and human EEG rhythms* p. 708. New York: Oxford University Press.

Ohara, S., Mima, T., Baba, K., Ikeda, A., Kunieda, T., Matsumoto, R., et al. (2001). Increased synchronization of cortical oscillatory activities between human supplementary motor and primary sensorimotor areas during voluntary movements. Journal of Neuroscience, *21*(23), 9377–9386.

Pfurtsheller, G., & Lopes da Silva, F. H. (1999). Event-related EEG/EMG synchronizations and desynchronization: basic principles. *Clinical Neurophysiology*, *110*, 1842–1857.

Salvador, R., Suckling, J., Coleman, M. R., Pickard, J. D., Menon, D., & Bullmore, E. (2005). Neurophysiological architecture of functional magnetic resonance images of human brain. *Cerebral Cortex*, *15*(9), 1332–1342.

Sporns, O., Chialvo, D. R., Kaiser, M., & Hilgetag, C. C. (2004). Organization, development and function of complex brain networks. *Trends in Cognitive Sciences*, *8*, 418–425.

Sporns, O., Tononi, G., & Edelman, G. E. (2000). Connectivity and complexity: the relationship between neuroanatomy and brain dynamics. *Neural Networks*, *13*, 909–922.

Sporns, O., & Zwi, J. D. (2004). The small world of the cerebral cortex. *Neuroinformatics*, *2*, 145–162.

Stam, C. J. (2004). Functional connectivity patterns of human magnetoencephalographic recordings: A 'small-world' network? *Neuroscience Letters*, *355*, 25–28.

Stam, C. J., Jones, B. F., Manshanden, I., van Cappellen van Walsum, A. M., Montez, T., Verbunt, J. P., et al. (2006a). Magnetoencephalographic evaluation of resting-state functional connectivity in Alzheimer's disease. *Neuroimage*, *32*, 1335–44.

Stam, C. J., Jones, B. F., Nolte, G., Breakspear, M., & Scheltens, P. (2006b). Small-world networks and functional connectivity in Alzheimer's disease. *Cerebral Cortex*, *17*, 92–99.

Stam, C. J., & Reijneveld, J. C. (2007). Graph theoretical analysis of complex networks in the brain. *Nonlinear Biomedical Physics*, *1*, 3.

Strogatz, S. H. (2001). Exploring complex networks. *Nature*, *410*, 268–276.

Tononi, G., Sporns, O., & Edelman, G. M. (1994). A measure for brain complexity: relating functional segregation and integration in the nervous system. *Proceedings of the National Academy of Sciences of the United States of America*, *91*, 5033–5037.

Watts, D. J., & Strogatz, S. H. (1998). Collective dynamics of 'small-world' networks. *Nature*, *393*, 440–442.

Yook, S. H., Jeong, H., Barabási, A., & Tu, Y. (2001). Weighted evolving networks. *Physical Review Letters*, *86*(25), 5835–5838.